AD-A094 104 ROME AIR DEVELOPMENT CENTER GRIFFISS AFB NY F/G 17/9
PREDICTION OF ELECTROMAGNETIC SCATTERING FOR ROUGH TERRAIN USIN--ETC(U)
SEP 80 R J PAPA, J F LENNON, R L TAYLOR
UNCLASSIFIED RADC-TR-80-289 NL

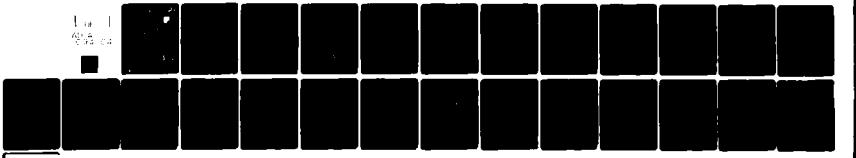

END
DATE FILMED
3-81
DTIC

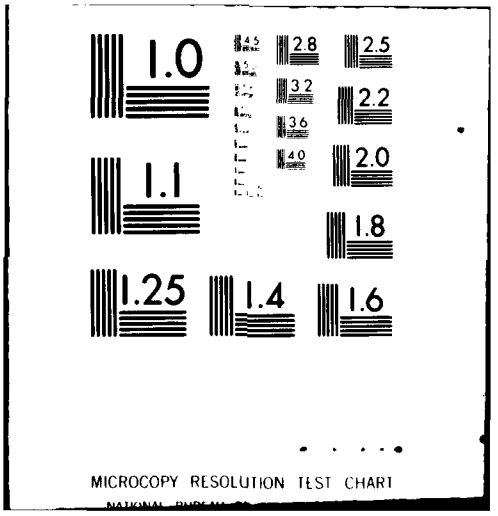
1.0
1.1
1.25
1.4
1.6
1.8
2.0
2.2
2.5
2.8
3.2
3.6
4.0
MICROCOPY RESOLUTION TEST CHART

LEVEL II

12

AD A094104

(14) RADC-TR-80-289
In-House Report
(11) Sep[redacted]80

(12) 25

(6) # PREDICTION OF ELECTROMAGNETIC SCATTERING FOR ROUGH TERRAIN USING STATISTICAL PARAMETERS DERIVED FROM DIGITIZED TOPOGRAPHIC MAPS,

(10) R. J. Papa
J. F. Lennon
R. L. Taylor

(16) 2305 (17) J4

ROME AIR DEVELOPMENT CENTER
Air Force Systems Command
Griffiss Air Force Base, New York 13441

This report has been reviewed by the RADC Public Affairs Office (PA) and is releasable to the National Technical Information Service (NTIS). At NTIS it will be releasable to the general public, including foreign nations.

RADC-TR-80-289 has been reviewed and is approved for publication.

APPROVED: John K. Schindler

JOHN K. SCHINDLER
Assistant Chief, EM Techniques Branch

APPROVED: Allan C. Schell

ALLAN C. SCHELL, Chief
Electromagnetic Sciences Division

FOR THE COMMANDER: John P. Huss

JOHN P. HUSS
Acting Chief, Plans Office

SUBJECT TO EXPORT CONTROL LAWS

This document contains information for manufacturing or using munitions of war. Export of the information contained herein, or release to foreign nationals within the United States, without first obtaining an export license, is a violation of the International Traffic in Arms Regulations. Such violation is subject to a penalty of up to 2 years imprisonment and a fine of $100,000 under 22 U.S.C 2778.

Include this notice with any reproduced portion of this document.

If your address has changed or if you wish to be removed from the RADC mailing list, or if the addressee is no longer employed by your organization, please notify RADC (EEC) Hanscom AFB MA 01731. This will assist us in maintaining a current mailing list.

Do not return this copy. Retain or destroy.

Unclassified

SECURITY CLASSIFICATION OF THIS PAGE (When Data Entered)

REPORT DOCUMENTATION PAGE	READ INSTRUCTIONS BEFORE COMPLETING FORM
1. REPORT NUMBER: RADC-TR-80-289	2. GOVT ACCESSION NO.: AD-A094104
3. RECIPIENT'S CATALOG NUMBER:	
4. TITLE (and Subtitle): PREDICTION OF ELECTROMAGNETIC SCATTERING FOR ROUGH TERRAIN USING STATISTICAL PARAMETERS DERIVED FROM DIGITIZED TOPOGRAPHIC MAPS	5. TYPE OF REPORT & PERIOD COVERED: In-House Report
	6. PERFORMING ORG. REPORT NUMBER:
7. AUTHOR(s): R. J. Papa, J. F. Lennon, R. L. Taylor	8. CONTRACT OR GRANT NUMBER(s):
9. PERFORMING ORGANIZATION NAME AND ADDRESS: Deputy for Electronic Technology (RADC/EEC), Hanscom AFB, Massachusetts 01731	10. PROGRAM ELEMENT, PROJECT, TASK AREA & WORK UNIT NUMBERS: 61102F, 2305J407
11. CONTROLLING OFFICE NAME AND ADDRESS: Deputy for Electronic Technology (RADC/EEC), Hanscom AFB, Massachusetts 01731	12. REPORT DATE: September 1980
	13. NUMBER OF PAGES: 24
14. MONITORING AGENCY NAME & ADDRESS (if different from Controlling Office)	15. SECURITY CLASS. (of this report): Unclassified
	15a. DECLASSIFICATION DOWNGRADING SCHEDULE

16. DISTRIBUTION STATEMENT (of this Report)

Approved for public release; distribution unlimited.

17. DISTRIBUTION STATEMENT (of the abstract entered in Block 20, if different from Report)

18. SUPPLEMENTARY NOTES

19. KEY WORDS (Continue on reverse side if necessary and identify by block number)

Radar multipath
Statistics
Terrain characterization

20. ABSTRACT (Continue on reverse side if necessary and identify by block number)

For terrain which is gently undulating and whose surface height excursions are large compared to a wavelength, well known formulas for the normalized bistatic cross section as a function of the polarization states of the incident and scattered EM waves are available in the literature. There are also several theoretical models which describe the EM scattering cross section of surfaces characterized by two scales of roughness. The present analysis applies parameter estimation techniques to a digitized topographic data base. The results are used in a hypothesis test to determine the best

DD FORM 1 JAN 73 1473 EDITION OF 1 NOV 65 IS OBSOLETE

Unclassified

SECURITY CLASSIFICATION OF THIS PAGE (When Data Entered)

20. (Cont)

probability density function (PDF) for the given map data. The accuracy of the analysis depends on the available data, the estimators employed, and the determination of appropriate PDF's. The example which will be discussed consists of a large number of terrain regions in an area of eastern Massachusetts. This area was chosen because experimental data in the form of electromagnetic forward scattering from the surface are available. Because of the number of cases involved, the complexity of the multivariate height distributions, and the type of measurements available, only a single observation of the multivariate data is used in the present analysis. The results of the statistical analysis for mean height, variance, correlation, PDF, and a geologic feature characterizing each subregion are presented. These are used in a single-roughness-scale electromagnetic scattering formulation to allow comparison with the experimental data. A computer program has been developed to determine the amount of specular and diffuse multipath power reaching a monopulse receiver from a pulsed beacon and the associated boresight pointing error. Terrain inhomogeneities and multiple specular reflection points are included in the analysis. Results are compared with data. Currently, the terrain analysis is being extended to apply to the two-scale theory for scattering with improved techniques for estimation of the statistical parameters of the scattering model.

Contents

Illustrations

Illustrations

Tables

Prediction of Electromagnetic Scattering for Rough Terrain Using Statistical Parameters Derived From Digitized Topographic Maps

I. INTRODUCTION

The characteristics of electromagnetic signals scattered from rough terrain include contributions from clutter return and multipath return.[1,2] These two aspects can be described by the theory of scattering from rough surfaces if properties of the terrain such as probability density function (PDF) for the surface height distribution, the covariance matrix, $\underset{\sim}{R}$, the variance in surface height, σ^2, and the complex dielectric constant characterizing the surface are known. The numerous theoretical models of EM wave scattering from rough surfaces, for example, Beckmann and Spizzichino,[1] Ruck et al,[2] Long,[3] and Brown,[4] all relate the normalized cross section of terrain to the foregoing parameters characterizing the rough surface.

In this report, the physical parameters of the rough surface are obtained from digitized terrain maps (furnished by the Electromagnetic Compatibility

(Received for publication 2 September 1980)

1. Beckmann, P., and Spizzichino, A. (1963) The Scattering of Electromagnetic Waves from Rough Surfaces, Macmillan Co.

2. Ruck, G.T., Barrick, D.E., Stuart, W.D., and Krichbaum, C.K. (1970) Radar Cross Section Handbook, Vol. 2, Plenum Press.

3. Long, M.W. (1975) Radar Reflectivity of Land and Sea, Lexington Books.

4. Brown, G.S. (1978) Backscattering from a Gaussian - distributed perfectly conducting rough surface, IEEE Trans. on Antennas and Prop. AP-26(No. 3):472.

Analysis Center, ECAC, and the Defense Mapping Agency, DMA). Estimation theory is employed to specify the corresponding statistical parameters. A hypothesis testing procedure determines the probability density function (PDF) for the surface heights.

The specific problem used as an example is that of characterizing a large terrain region considered to be made up of smaller subareas (~ 4 km^2). The main feature of interest is the distribution of heights within these subregions. Each subregion is characterized by a geologic code and several statistical parameters. In particular, we are concerned with being able to associate a PDF with the range of heights (z_i) in the subregions and to determine parameters that make the general PDF explicit. The data elements $z_i = z_i(x_k, y_\ell)$, where $i = 1, 2, 3, \ldots N$, and N is the total number of grid points in the x - y plane constituting the subregion. Here, x_k denotes the k^{th} equally spaced x-value along the x-axis and y_ℓ denotes the ℓ^{th} y-value along the y-axis, where $k = 1, 2, \ldots \sqrt{N}$ and $\ell = 1, 2, \ldots \sqrt{N}$. Thus, the N points are distributed in the x-y plane in order to form a rectangular grid. The covariance matrix can be assumed to have the form:

$$R_{mn} = \sigma^2 \exp\left(-\tau_{mn}^2/T^2\right)$$

where T is the correlation length and for this class of data sets, the form of τ_{mn} is

$$\tau_{mn}^2 = (x_m - x_n)^2 + (y_m - y_n)^2 .$$

The motivation for assuming a covariance matrix of this form is that it leads to a tractable mathematical expression for the incoherent power scattered when an electromagnetic wave is reflected from a rough surface. Similarly, in the hypothesis testing procedure, the binary decision process involves the case where the PDF is either an N-variate Gaussian or exponential. This specialization is also motivated by the theory of electromagnetic wave scattering from rough surfaces.[1,2]

The normalized radar cross section of the rough surface used in this report was derived by Hagfors,[6] Barrick,[7] and Semenov.[8] This cross section, σ_o, is

5. Whalen, A. D. (1971) Detection of Signals in Noise, Academic Press.
6. Hagfors, T. (1964) Backscattering from an undulating surface with applications to radar returns from the moon, J. Geophys. Res. 69:3779.
7. Barrick, D. E. (1968) Relationship between slope probability density function and the physical optics integral in rough surface scattering, Proc. IEEE 56:1728.
8. Semenov, B. (1965) Scattering of electromagnetic waves from restricted portions of rough surfaces with finite conductivity, Radiotekh. i Elektron, 10:1952.

incorporated into a computer program which calculates the amount of specular and diffuse multipath power entering a monopulse receiver from a beacon located over rough terrain (see Figure 1). The computer program also calculates the error in boresight pointing accuracy of a monopulse receiving antenna due to noise and diffuse multipath. Among other things, the computer program takes into consideration, (1) the spatial nonuniformity of the rough earth (that is, the preceding characterization parameters), (2) nonuniformities in the glistening surface, (3) finite pulse length of the beacon, (4) antenna elevation power pattern of the monopulse receiver, (5) multiple specular reflection points due to unevenness in surface height, (6) interference between direct signal and multiple specularly reflected signals, and (7) finite azimuthal beamwidth of transmitter and receiver. Finally, for the case of normally distributed surface heights, Sancer's[9] results are employed to describe the effects of shadowing and Brown's[10] general backscatter shadowing results have been extended to handle the exponential case.

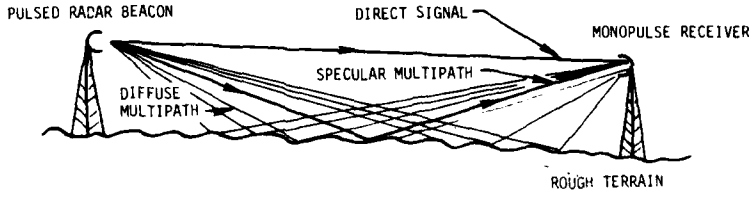

Figure 1. Reflection of Radar Waves From Rough Terrain

The results of the program describe the effect of the terrain on the electromagnetic signal. The final outputs include total coherent and diffuse power levels, and the induced boresight error. The data output from the computer program for the sum pattern coherent power and angular error in boresight is compared with experimental data taken by personnel at the MIT Lincoln Laboratory Discrete Address Beacon System (DABS) test site.[11]

9. Sancer, M.I. (1969) Shadow-corrected electromagnetic scattering from a randomly rough surface, IEEE Trans. on Antennas and Prop. AP-17:577-585.

10. Brown, G.S. (1980) Shadowing by non-Gaussian random surfaces, Proceedings of the Second Workshop on Terrain and Sea Scatter, George Washington University, Washington, D.C.

11. McGarty, T.P. (1975) The Statistical Characteristics of Diffuse Multipath and its Effect on Antenna Performance, AD-009869.

2. STATISTICAL ANALYSIS

In our statistical analysis of terrain heights, we carry out a series of operations: First, we propose some multivariate probability density functions that may represent the observed distribution of height values; next we use the available data to generate appropriate estimators of the parameters of the respective densities; finally, we conduct a hypothesis test to ascertain which density function is more likely to have produced the observed height data.

The two PDF's for the heights are multivariate Gaussian or exponential. The Gaussian has a well-known form:[12]

$$P_G(z_1', z_2', \ldots, z_N') = \left[(2\pi)^{N/2} |\underset{\sim}{R}|^{1/2}\right]^{-1} \exp\left[-\frac{1}{2}(\underset{\sim}{z}' - \underset{\sim}{\mu})^T \underset{\sim}{R}^{-1} (\underset{\sim}{z}' - \underset{\sim}{\mu})\right],$$

where $\underset{\sim}{R}$ represents the covariance matrix. For our case, we assume equal means ($\underset{\sim}{\mu}$), variances (σ^2) and that the correlation function ($\rho_{ij} = \sigma_{ij}/\sigma^2$) has a Gaussian dependence on the separation between points. The next aspect is to develop a similar form for the exponential:

$$P_E(z_1', z_2', \ldots,) = C_1 \exp\left\{-C_2\left[(\underset{\sim}{z}' - \underset{\sim}{\mu})^T \underset{\sim}{R}^{-1} (\underset{\sim}{z}' - \underset{\sim}{\mu})\right]^{1/2}\right\}$$

The two coefficients (C_1, C_2) have to be determined. This will result in a form that satisfies the requirements for a PDF. To evaluate the coefficients, we use the properties that the zeroth moment integral of a PDF is equal to unity and the second moment integral is equal to the variance. We thus obtain a form for the multivariate exponential:

$$P_E(z_1', z_2', \ldots z_N') = \left[2^{\frac{N+1}{2}} (2\pi)^{\frac{N-1}{2}} \Gamma\left(\frac{N+1}{2}\right) |R|^{1/2}\right]^{-1}$$
$$(N+1)^{N/2} \exp\left\{-\left[(N+1)(\underset{\sim}{z}' - \underset{\sim}{\mu})^T \underset{\sim}{R}^{-1} (\underset{\sim}{z}' - \underset{\sim}{\mu})\right]^{1/2}\right\}$$

In order to decide which of these two PDF's is more appropriate for the data, we must next establish estimators for the parameters of the densities: the means, variance, and covariances. The complexity of correlated multivariate analysis and the computational limitations associated with the available data formats caused us to select estimators that have an intuitive appeal based on their form rather than a rigorous derivation. From our assumption of equal means and variances, we use the sample mean as the estimator for the mean height and the sample variance as the variance estimate:

12. Mood, A. M., and Graybill, F. A. (1963) Introduction to the Theory of Statistics, McGraw-Hill.

$$\hat{\bar{z}} = (1/N) \sum_{i=1}^{\sqrt{N}} \sum_{n=1}^{\sqrt{N}} z(x_i, y_j) \quad \text{(mean) and}$$

$$\hat{\sigma}^2 = (1/N) \sum_{i=1}^{\sqrt{N}} \sum_{j=1}^{\sqrt{N}} (z_{ij} - \hat{\bar{z}})^2 \quad \text{(variance).}$$

The procedure for the covariance matrix estimator is more complicated. A correlation length, T, is defined as the separation at which a normalized covariance function C_{zz} has decreased to the value e^{-1}, where $C_{zz} = \gamma_{zz}/\sigma^2$, and γ_{zz} is the estimator for the covariance. The data are used to determine the estimate of T in this fashion and then the complete covariance estimator is formed from the relation:

$$\gamma_{zz}(m,n) = \hat{\sigma}^2 \exp\left(-\tau_{mn}^2/T^2\right)$$

(separate X and Y relations are calculated). The form of the covariance (X direction) used to determine T is

$$C_{zz}(k) = (1/N\hat{\sigma}^2)\left[\sum_{j=1}^{\sqrt{N}} \sum_{i=1}^{\sqrt{N}-k} Z_{ij} Z_{i+kj} - \hat{\bar{z}} \sum_{j=1}^{\sqrt{N}} \sum_{i=1}^{\sqrt{N}-k} Z_{ij} - \frac{k\hat{\bar{z}}^2}{\sqrt{N}} \right]$$

where k represents the separation distance. A least squares fit of the C_{zz} values to a parabola is then used to find T. Under the assumptions that have been made, the above estimators are similar to those found in Jenkins and Watts.[13] After obtaining the values for T in the X and Y directions, the two values are averaged to find the final estimate of T in a given subregion.

We now have the two PDF forms and the parameters required for them. The next aspect is to decide which PDF is the more appropriate for the given data. One final comment on the parameters should be made. In order to satisfy the restrictions of the PDF's, it is necessary to show that the quadratic form appearing in both cases is positive definite. This has been demonstrated for the above cases by making use of the Gaussian form assigned to the covariance matrix elements. Details can be found in the report by Lennon and Papa.[14]

The form of the hypothesis test used here is based on the maximum a posteriori probability criterion. This is equivalent to a minimum error probability criterion. We assign hypothesis H_1 to the Gaussian case and hypothesis H_o to the exponential. Then the likelihood ratio parameter,

---

13. Jenkins, G.M., and Watts, D.G. (1968) Spectral Analysis and its Applications, Holden-Day.

14. Lennon, J.F., and Papa, R.J. (1980) Statistical Characterization of Rough Terrain, RADC-TR-80-9, RADC/EE Hanscom AFB, Massachusetts.

$$\lambda \triangleq \frac{P_1(z_1, z_2, \cdots, z_N)}{P_0(z_1, z_2, \cdots, z_N)} .$$

Let $P(H_o)$ be the probability that hypothesis H_o is true. Then the decision rule may be written as: Choose H_1 if

$$\lambda \geq \frac{P(H_o)}{1 - P(H_o)} .$$

For our case, we assume that it is equally probable that hypothesis H_1 or H_o is true and the decision rule reduces to whether or not $\lambda \geq 1$. Note that it may be possible to alter the probability that H_o is true based on external evidence (such as the type of terrain).

When the specific forms for the two PDF's are introduced into this relation it becomes

$$\lambda = \frac{P_1}{P_o} = \left(\frac{\Gamma\left(\frac{N+1}{2}\right) e^{\left(\frac{N+1}{2}\right)}}{\sqrt{\pi}\left(\frac{N+1}{2}\right)^{N/2}} \right) \exp\left(-\frac{1}{2} (Q - \sqrt{N+1})^2 \right)$$

where

$$Q = \left[(\underset{\sim}{z} - \underset{\sim}{\mu})^T \underset{\sim}{R}^{-1} (\underset{\sim}{z} - \underset{\sim}{\mu}) \right]^{1/2} .$$

For convenience we rewrite the test in logarithmic form and obtain the result that H_1 is true if

$$Q \leq \left\{ \left[2 \ln\left(\Gamma\left(\frac{N+1}{2}\right)\right) + (N+1) - \ln \pi - N \ln\left(\frac{N+1}{2}\right) \right]^{1/2} + \sqrt{N+1} \right\}$$

or

$$Q \geq \left\{ \sqrt{N+1} - \left[2 \ln\left(\Gamma\left(\frac{N+1}{2}\right)\right) + (N+1) - \ln \pi - N \ln\left(\frac{N+1}{2}\right) \right]^{1/2} \right\} .$$

For the actual cases $N = 100$ and the specific result is that we decide that the terrain heights in a given region are from a Gaussian PDF if

$$85.01 \leq \left[(\underset{\sim}{z} - \underset{\sim}{\mu})^T \underset{\sim}{R}^{-1} (\underset{\sim}{z} - \underset{\sim}{\mu}) \right] \leq 118.37$$

and conversely the points are exponential if $Q^2 > 118.27$ or $Q^2 < 85.01$.

These procedures have been applied to a specific site to allow comparison of theoretical electromagnetic calculations based on the terrain characterization with actual experimental data available for the territory described.

3. SITE CHARACTERIZATION

The specific site used for the characterization is in eastern Massachusetts.[11] Because of the availability of data on electromagnetic scattering from that terrain, this area was selected to compare theoretical calculations with experimental results. A rectangular region around this Discrete Address Beacon System (DABS) site was designated. The area was 47.3 km long and 42.2 km wide. It was subdivided into smaller rectangular cells, each with sides of 2050 m by 1852 m, with a further subdivision of each cell into a 10 × 10 grid of points. A data base of topographic elevations for this area is available at the Electromagnetic Compatibility Analysis Center (ECAC), prepared from Defense Mapping Agency (DMA) supplied digitized terrain maps at 1:250,000 scale size.

The statistical data for each cell has been recorded on a computer tape for use with the program for the electromagnetic analysis. Each cell is represented by seven descriptors. The first two entries are the (X, Y) coordinates for the center of the cell (the origin of the coordinate system is taken as the center of the extreme southwestern corner of the rectangular region). The next item is the geological code for the cell. The predominant feature is woods; there are a number of cells containing clusters of lakes and ponds and a few town sites with associated cleared areas. This is followed by the mean and variance of the heights in the cell and the estimated correlation length T. The units of length are in meters. The final quantity is the result of the hypothesis test. This result is presented in a format such that the heights in a region are Gaussian when $-33.36 < \text{TEST} < 0$. When TEST = 0 and the variance is very small, the region is essentially a smooth surface (no roughness).

When the overall results for the region are examined,[14] one observes that when the magnitude of TEST is very large, correlation length is also large, and for those cases, T is comparable to one-half the cell size or even larger. When this occurs, the determinant of the covariance matrix $\underset{\sim}{R}$ becomes very small. As a result, it becomes more difficult to obtain an accurate inverse of $\underset{\sim}{R}$ due to rapid build-up of round-off error. A related difficulty is that for some cases TEST < − 118.37. This would be possible only if the quadratic form Q^2 is not positive definite. Thus, further machine-induced errors are present, and those results can not be considered valid. Further consideration is being given to the statistical aspects.

In order to use these results in the rough surface electromagnetic calculations, one additional aspect should be noted. For the types of geological features that describe the respective regions, data exists on the associated complex dielectric constants at microwave frequencies.[15,3]

---

15. Lytle, R.J. (1974) Measurement of earth medium electrical characteristics: techniques, results and applications, IEEE Trans on Geoscience Electronics GE-12:81.

4. ELECTROMAGNETIC SCATTERING ANALYSIS

The radar cross section of terrain is normalized with respect to the average area illuminated by the radar, A. The normalized cross section σ_o may be divided into three general categories: (1) The slightly rough surface;[16] (2) the very rough surface;[1,6,7,8] and (3) the multiple scale rough surface.[17,18,4] This report is concerned with the second category, that is, the very rough surface.

Ruck et al[2] give expressions for the average bistatic rough surface cross section σ_o under the following four assumptions: (1) the radius of curvature of the surface irregularities is larger than a wavelength; (2) the roughness is isotropic in both surface dimensions; (3) the correlation length is smaller than either the X or Y dimension of the sample subregion; and (4) multiple scattering is neglected. Using the notation of Ruck et al[2] one notes that the expression for σ_o becomes:

$$\sigma_o = |\beta_{pq}|^2 J$$

where

$$J = \frac{T^2}{\sigma^2 \xi_Z^2} \exp\left[-\left(\frac{T^2}{4\sigma^2}\right)\left(\frac{\xi_X^2 + \xi_Y^2}{\xi_Z^2}\right)\right]$$

for a Gaussian bivariate surface height probability density function and

$$J = \frac{3T^2}{\sigma^2 \xi_Z^2} \exp\left[-\left(\frac{\sqrt{6}\,T}{2\sigma}\right)\left(\frac{\xi_X^2 + \xi_Y^2}{\xi_Z^2}\right)^{1/2}\right]$$

for an exponential surface height probability density function. The scattering matrix elements β_{pq} are given by

$$\beta_{VV} = \frac{(1 + \cos 2\alpha)\, R_{\parallel}(\alpha)}{(\cos\theta_i + \cos\theta_s)} \quad \text{(vertical polarization)}$$

16. Peake, W. H. (1959) The interaction of Electromagnetic Waves with Some Natural Surfaces, Antenna Laboratory, Ohio State University Report No. 898-2.

17. Wright, J. W. (1968) A new model for sea clutter, IEEE Trans. on Antennas and Prop. AP-16:217-223.

18. Fuks, I. (1966) Contributation to the theory of radio wave scattering on the perturbed sea surface, Iz. Vyssh. Ucheb. Zaved. Radiofiz 5:876.

$$\beta_{hh} = -\frac{(1 + \cos 2\alpha)\, R_{\perp}(\alpha)}{(\cos\theta_i + \cos\theta_s)} \qquad \text{(horizontal polarization)}$$

$$R_{||}(\alpha) = \frac{\epsilon_r \cos\alpha - \sqrt{\epsilon_r - \sin^2\alpha}}{\epsilon_r \cos\alpha + \sqrt{\epsilon_r - \sin^2\alpha}}$$

$$R_{\perp}(\alpha) = \frac{\cos\alpha - \sqrt{\epsilon_r - \sin^2\alpha}}{\cos\alpha + \sqrt{\epsilon_r - \sin^2\alpha}}$$

where

θ_i = angle of incidence (with respect to surface normal)

θ_s = angle of scattering (with respect to surface normal)

$\xi_x = \sin\theta_i - \sin\theta_s, \quad \xi_y = 0.0, \quad \xi_z = -\cos\theta_i - 1.0,$

and

$$\alpha = \left(\frac{\theta_i + \theta_s}{2}\right).$$

Here, ϵ_r is the relative complex dielectric constant of the surface, the subscript $||$ refers to the E-field in the plane of incidence, and the subscript $\perp$ refers to the E-field normal to the plane of incidence. These simplified forms of Ruck's expression follow from the assumption that the receiver is far from the transmitter so that the portion of the "glistening surface"[1] that contributes to the diffuse multipath is a long, narrow strip extending between the transmitter and receiver. This assumption allows us to make the approximation that the azimuthal scattering angle $\phi_s \approx 0.0$. To describe the effect of shadowing, the previous expression for σ_o is multiplied by the appropriate shadowing function.

It was explained in the Introduction how a computer program was developed to incorporate the expression for σ_o into an integral over the glistening surface. In order to calculate the amount of coherent power (specular plus direct) and diffuse multipath power reaching a monopulse receiver from a beacon located over rough terrain (see Figure 1), the computer program uses the previously described data tape of the statistical parameters for a particular site as an input. Other input variables characterize the transmitter, the environmental aspects, and the receiver. Transmitter values include the gain of the transmitter, the polarization of the transmitted wave, the peak power of the transmitted pulse, the pulse length, and the wavelength of the signal. External inputs include the complex dielectric

constant of each type of geological region, the coordinates (latitude and longitude) of the monopulse receiver, the initial and final position of the aircraft containing the transmitter, a parameter to control the effects of shadowing, and the velocity of the aircraft. Receiver data are the height of the receiver, the bandwidth of the receiver, the front-end receiver-noise figure, the antenna gain for the sum and difference patterns of the monopulse receiver, its azimuthal beamwidth, the sampling frequency of the receiver, the transmission line loss factor of the cables connecting the antenna to receiver, and the difference pattern slope near the boresight axis.

From a knowledge of the initial and final positions of the aircraft and the aircraft speed, the computer program first calculates the trajectory, as a function of time. Then, from a modified form of the radar range equation, the electric field intensity of the direct signal at the receiver is calculated at fixed time intervals (sampling time is an input variable to the program). For the specular multipath rays, all possible specular reflection points between the transmitter and receiver are determined for each position of the transmitter. Multiple specular reflection points due to unevenness in surface height and possible ray blocking are taken into consideration. The finite dielectric constant of the earth at each specular point, the antenna elevation pattern (receive), and the surface roughness are also accounted for in calculating the phase and amplitude of each specular multipath ray. At each point on the transmitter's trajectory, the total coherent power for the sum and difference channels in the monopulse receiver is calculated. Various assumptions on the roughness effects have been examined. These are discussed in Section 5.

The diffuse multipath power, P_{Diff} entering the receiver is obtained from the equation

$$P_{Diff} = \frac{P_T G_{TR}^{AZ} G_R^{AZ} \lambda^2}{(4\pi)^3} \iint \frac{G_{TR}^{EL}(\theta_1) G_R^{EL}(\theta_2) \sigma_o}{R_1^2 R_2^2} \, dS$$

where

P_T = transmitted power,

λ = wavelength,

G_{TR}^{AZ} = gain (power) of transmitter in azimuth,

G_R^{AZ} = gain of receiver in azimuth,

G_{RT}^{EL} = gain of transmitter in elevation,

$G_R^{(1)}$ = [illegible] receiver [illegible],

θ_1 = angle between boresight and point on glistening surface for transmitter,

θ_2 = angle between boresight and point on glistening surface for receiver,

R_1 = range between transmitter and point on glistening surface,

R_2 = range between receiver and point on glistening surface,

dS = element of area of glistening surface which is illuminated by beacon.

In the numerical integration of the equation for P_{Diff}, account is taken of spatial inhomogeneities of the rough earth, nonuniformities in the boundaries of the glistening surface, and the size of the footprint on the uneven terrain due to finite pulse length and azimuthal beamwidth.

To calculate the error in boresight of the monopulse receiver due to diffuse multipath and receiver noise, it is assumed that the diffuse multipath is decorrelated from pulse to pulse, and that the spectral width of the diffuse multipath power is narrow compared to the bandwidth of the receiver processor. These assumptions appear to be justified on the basis of rough, order-of-magnitude estimates of the appropriate parameters. Under these assumptions, the total amount of noise like interference is given by

$$N_I = P_{Diff} + N_o,$$

where

N_I = noiselike interference power,

N_o = noise power from environment plus receiver.

The error, σ_θ, in azimuthal boresight pointing accuracy is given by the expression:[19]

$$\sigma_\theta = \frac{\theta_B}{k_m \sqrt{2\ STIR}}$$

19. Barton, D.K., and Ward, H.R. (1969) Handbook of Radar Measurement, Prentice-Hall.

where

θ_B = azimuthal beamwidth,

STIR P_{coh}/N_I = signal to interference ratio in the difference channel,

P_{coh} = coherent power in sum channel,

k_m = normalized monopulse slope (obtainable from sum and difference patterns).

The output of the computer program consists of azimuthal angular error in boresight due to noise, the error due to noise plus diffuse multipath, the total sum pattern coherent power, the total diffuse power, signal-to-noise ratio, signal-to-interference ratio, and range from transmitter to receiver. In the conclusions, the computer output for the analysis of a particular site is compared with some experimental data.

5. RESULTS AND CONCLUSIONS

Two theoretical results, the coherent power in the sum channel of a monopulse antenna, P_{coh}, and the standard deviation in boresight pointing accuracy, σ_θ, are compared with the experimental data of McGarty,[11] taken at the Discrete Address Beacon System (DABS) site.

The DABS receiver was an L-band rotatable array. The beacon was located on a U-10 aircraft which flew a number of radial trajectories toward and away from the monopulse receiver. Data were recorded for about 100 flights for different aircraft heights, different radial flight trajectories, and different receiver-antenna tilt angles. The conditions under which the data were taken are listed in Table 1.

In order to make the comparisons, various manipulations were required. In the equation for σ_θ, the normalized slope in the difference pattern near boresight k_m was obtained from graphs of the sum and difference patterns of the monopulse antenna. Within the accuracy of these graphs, it appears that $1.5 \leq k_m \leq 1.7$. Also, instead of integrating the difference pattern in azimuth over the glistening surface to obtain the diffuse multipath power received, an average value (18.5 dB) for the difference channel gain was used over a 3° beamwidth.

Table 1. Experimental Conditions for Discrete Address Beacon System Tests

Front end receiver noise figure	3 dB
Gain of monopulse receiver (sum pattern)	22.5 dB
Gain of transmitter	4 dB
Height of receiver	101 m
Height of transmitter	1220 m
Signal polarization	vertical
Peak transmitter power	350 W
Pulse length	20 μsec
Azimuthal beamwidth (receiver)	3°
Wavelength	0.275 m
Transmission line loss factor	3 dB

The experimental results are illustrated in Figures 2 and 3. Figure 2 is a plot of the sum signal (P_{coh}) versus range of transmitter to receiver in nmi. Figure 3 is a plot of azimuth error (σ_θ) versus range in nmi.

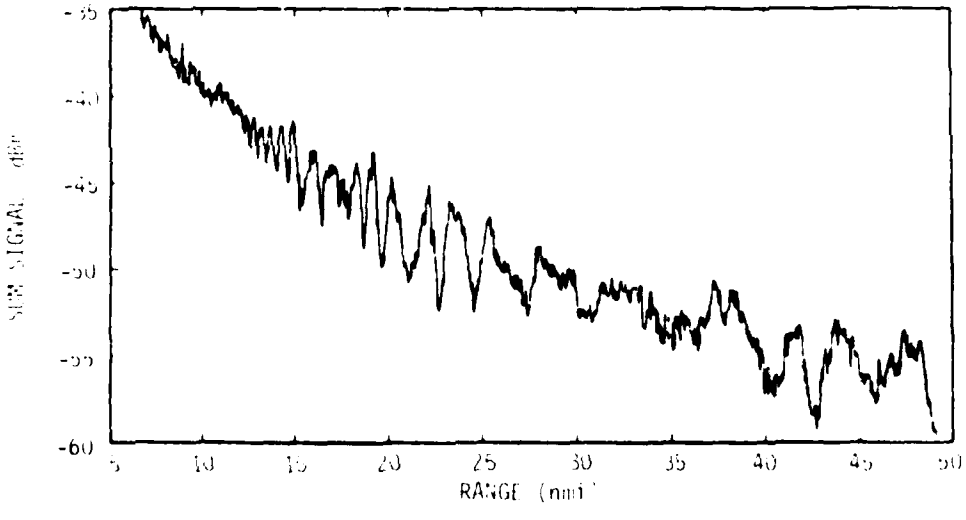

Figure 2. Experimental Data: Sum Signal (P_{coh}) vs Range

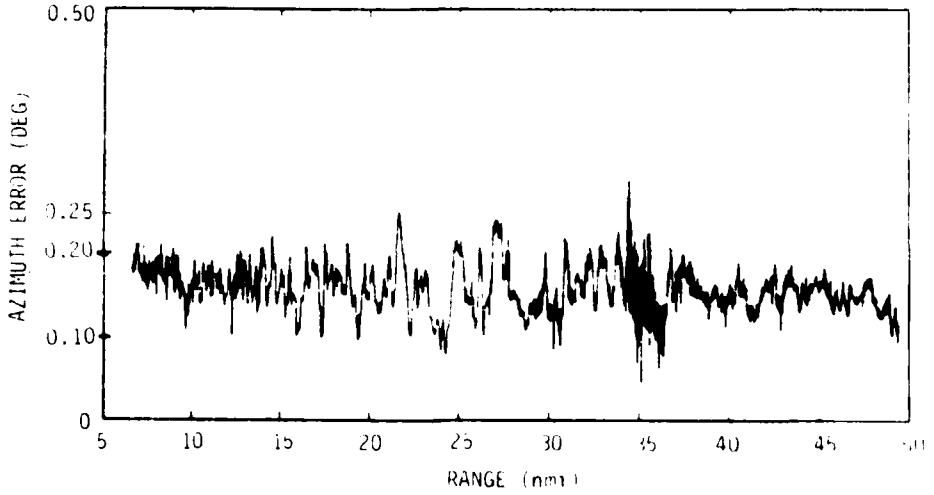

Figure 3. Experimental Data: Azimuth Error (σ_θ) vs Range

When the variance associated with the distribution of heights over the whole region is used, the coherent power from the specular rays is minimal and the result is just the expected direct ray fall-off of power with range. This is consistent with the scale of the actual contributing region (on the order of the first Fresnel zone) and the corresponding assumptions of small correlation length in the scattering formulation. The use of more localized variances associated with the Fresnel zone dimensions produces more multipath effects. Figure 4 shows the calculated power for the sum-signal, together with the actual data. The specular contributions come from three areas and the effect of the different local variances assigned to each can be seen in the changing behavior of the signal along the trajectory. It should be noted that the theoretical results tend to be about 6 dB higher on the average, probably due to the fact that the processing losses are unknown and hence have been neglected. Figure 5 represents an attempt to correct for this effect by introducing a total processing loss of -5 dB.

The next figures show the results for calculated boresight error when both extremes for k_m are used and different assumptions made as to shadowing and the PDF of the terrain heights. For the particular trajectory of the experiment, the statistical analysis indicates that in all the terrain regions contributing to the calculations, the heights are best described as being from exponential distributions.

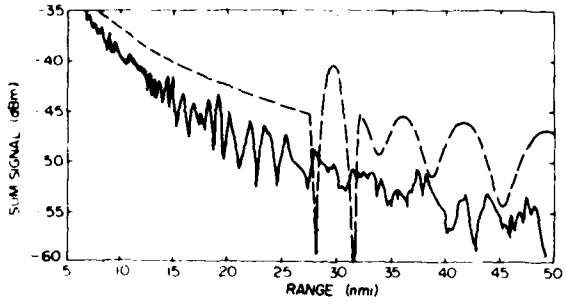

Figure 4. Sum Signal (P_{coh}) vs Range: Theoretical Results Without Processing Losses (---) and Experimental Data (—)

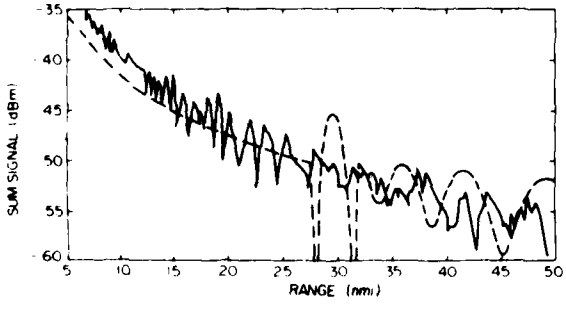

Figure 5. Sum Signal (P_{coh}) vs Range: Theoretical Results With Typical Processing Losses (---) and Experimental Data (—)

In Figure 6, $k_m = 1.5$ and the results for shadowing are shown for the case where processing losses are included. Comparison of Figure 6 with Figure 3 shows that the theoretical boresight errors σ_θ are less than the experimental values. This may be attributable to not integrating the true monopulse difference pattern in azimuth over the entire glistening surface. Our use of an average 18.5 dB gain over a 3° beamwidth may have resulted in less received diffuse multipath power. Two factors neglected in the program can lead to increased boresight error. These are the azimuthal variation in σ_θ and the fine scale surface roughness contribution. However, even the present agreement between theory and experiment is reasonably good. It may be noted that shadowing reduces the error σ_θ only a very small amount for the system parameters of this report.

Next we show the results for $k_m = 1.7$. Figure 7 shows the boresight error for an exponential surface including the effect of shadowing. Comparison with Figure 3 shows that the higher value for k_m results in slightly poorer agreement between theory and experiment. The conclusion is that for the range of k_m values used here, there is no significant effect on σ_θ. To complete the analysis of the effect of PDF, we have the case where all the subregions are assumed to have Gaussian distributed surface heights with $k_m = 1.5$. These results are shown in Figure 8. Comparison with Figure 6 indicates that the assumption that the surface heights

are all normally distributed, results in less diffuse multipath power entering the receiver. This represents poorer agreement with the data.

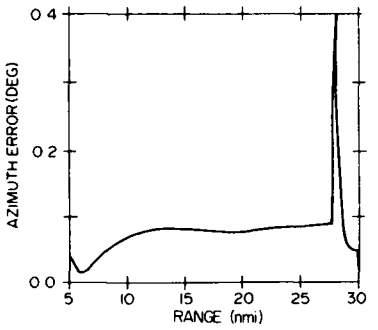

Figure 6. Theoretical Calculations: σ_θ vs Range: k_m = 1.5, Shadowing (Actual Exponential Heights)

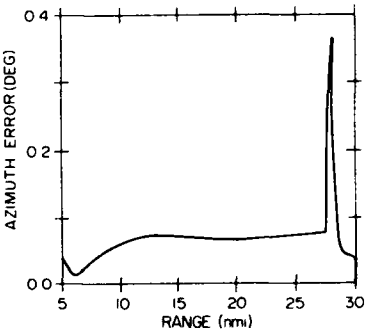

Figure 7. Theoretical Calculations: σ_θ vs Range: k_m = 1.7, Shadowing (Actual Exponential Heights)

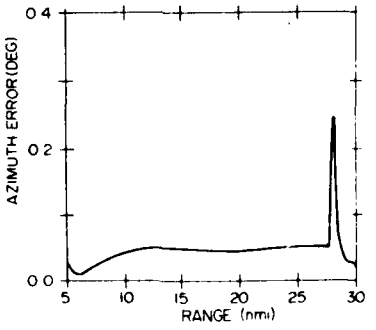

Figure 8. Theoretical Calculations: σ_θ vs Range: k_m = 1.5, Shadowing (Assumed Gaussian Heights)

McGarty also made some comparisons between the experimental data and theoretical calculations based on the rough surface scattering model proposed by Barrick.[20] McGarty's work involved the use of the channel spread function, which

20. Barrick, D. E. (1968) Rough surface scattering based on the specular point theory, IEEE Trans. on Antennas and Prop. AP-16:449-454.

takes into consideration the fact that the diffuse multipath power has a wavenumber spectrum associated with it. His results show reasonably good agreement between theory and experiment, but there is no discussion of how the surface correlation length and the variance in surface height were estimated.

The results presented in this report are being extended. The average power restriction is being relaxed. Better techniques for statistical parameter estimation of terrain features and alternative methods for the hypothesis testing procedure are being pursued. Finally, the effects of mean surface tilt for each subregion and theoretical models of σ_θ which contain multiple scales of surface roughness will be included in the scattering model.

References

1. Beckmann, P., and Spizzichino, A. (1963) The Scattering of Electromagnetic Waves from Rough Surfaces, Macmillan Co.
2. Ruck, G.T., Barrick, D.E., Stuart, W.D., and Krichbaum, C.K. (1970) Radar Cross Section Handbook, Vol. 2, Plenum Press.
3. Long, M.W. (1975) Radar Reflectivity of Land and Sea, Lexington Books.
4. Brown, G.S. (1978) Backscattering from a Gaussian - distributed perfectly conducting rough surface, IEEE Trans. on Antennas and Prop. AP-26(No. 3):472.
5. Whalen, A.D. (1971) Detection of Signals in Noise, Academic Press.
6. Hagfors, T. (1964) Backscattering from an undulating surface with applications to radar returns from the moon, J. Geophys. Res. 69:3779.
7. Barrick, D.E. (1968) Relationship between slope probability density function and the physical optics integral in rough surface scattering, Proc. IEEE 56:1728.
8. Semenov, B. (1965) Scattering of electromagnetic waves from restricted portions of rough surfaces with finite conductivity, Radiotekh. i Elektron, 10:1952.
9. Sancer, M.I. (1969) Shadow-corrected electromagnetic scattering from a randomly rough surface, IEEE Trans. on Antennas and Prop. AP-17:577-585.
10. Brown, G.S. (1980) Shadowing by non-Gaussian random surfaces, Proceedings of the Second Workshop on Terrain and Sea Scatter, George Washington University, Washington, D.C.
11. McGarty, T.P. (1975) The Statistical Characteristics of Diffuse Multipath and its Effect on Antenna Performance, AD-A009869.
12. Mood, A.M., and Graybill, F.A. (1963) Introduction to the Theory of Statistics, McGraw-Hill.
13. Jenkins, G.M., and Watts, D.G. (1968) Spectral Analysis and its Applications, Holden-Day.

14. Lennon, J. F., and Papa, R. J. (1980) Statistical Characterization of Rough Terrain, RADC-TR-80-9, RADC/EE Hanscom AFB, Massachusetts.

15. Lytle, R. J. (1974) Measurement of earth medium electrical characteristics: techniques, results and applications, IEEE Trans. on Geoscience Electronics GE-12:81.

16. Peake, W. H. (1959) The Interaction of Electromagnetic Waves with Some Natural Surfaces, Antenna Laboratory, Ohio State University, Report No. 898-2.

17. Wright, J. W. (1968) A new model for sea clutter, IEEE Trans. on Antennas and Prop. AP-16:217-223.

18. Fuks, I. (1966) Contribution to the theory of radio wave scattering on the perturbed sea surface, Izv. Vyssh. Ucheb. Zaved. Radiofiz 5:876.

19. Barton, D. K, and Ward, H. R. (1969) Handbook of Radar Measurement, Prentice-Hall.

20. Barrick, D. E. (1968) Rough surface scattering based on the specular point theory, IEEE Trans. on Antennas and Prop. AP-16:449-454.

MISSION
of
Rome Air Development Center

RADC plans and executes research, development, test and selected acquisition programs in support of Command, Control Communications and Intelligence (C^3I) activities. Technical and engineering support within areas of technical competence is provided to ESD Program Offices (POs) and other ESD elements. The principal technical mission areas are communications, electromagnetic guidance and control, surveillance of ground and aerospace objects, intelligence data collection and handling, information system technology, ionospheric propagation, solid state sciences, microwave physics and electronic reliability, maintainability and compatibility.

Printed by
United States Air Force
Hanscom AFB, Mass. 01731